Article ID: 1000-7032(2018)05-0615-06

Spectral Parameter Calculation of Ho^{3+}, Tm^{3+} Co-doped $KYb(WO_4)_2$ Laser Crystal

BI Lin[1*], DI Xiao-qiang[1], ZHAO Jian-ping[1], LI Chun[2], LIU Jing-he[2]

(1. *School of Computer Science and Technology, Changchun University of Science and Technology, Changchun* 130022, *China*;
2. *School of Materials Science and Engineering, Changchun University of Science and Technology, Changchun* 130022, *China*)

* *Corresponding Author, E-mail: bilin*7080@163.*com*

Abstract: $KHo_{0.04}Tm_{0.06}Yb_{0.9}(WO_4)_2$ laser crystal was grown by the top seeded solution growth (TSSG) method. The absorption and fluorescent spectra of the crystal were measured, and the spectral parameters were calculated, too. The experimental results show that there is a broader absorption band at the range of 890 – 1 000 nm with a full width at half maximum (FWHM) of 90 nm. The absorption cross section of main emission peak at 1 000 nm is 16.92×10^{-20} cm^2. Meanwhile, Tm^{3+} ions in the crystal have a wider absorption band at 1 690 – 1 812 nm with a FWHM of 118 nm. Therefore, the energy transfer of Yb→Ho, Yb→Tm, Tm→Ho can be easily achieved. The spectral strength parameters of the crystal were calculated based on the Judd-Ofelt theory. According to the energy level diagram of Tm^{3+}, Ho^{3+} and Yb^{3+} ions, three kinds of energy transfer modes at 1 750 – 2 200 nm emission were discussed. The stimulated emission cross section of main emission peak at 2 030 nm is 3.47×10^{-20} cm^2, which indicates that the crystal can be used as an excellent laser gain medium at the range of 2 μm.

Key words: $KHo_{0.04}Tm_{0.06}Yb_{0.9}(WO_4)_2$ laser crystal; absorption spectrum; fluorescent spectrum; spectral parameter calculation

CLC number: O482.31 **Document code**: A **DOI**: 10.3788/fgxb20183905.0615

钬铥双掺钨酸镱钾激光晶体光谱参数计算

毕 琳[1*], 底晓强[1], 赵建平[1], 李 春[2], 刘景和[2]

(1. 长春理工大学 计算机科学技术学院, 吉林 长春 130022; 2. 长春理工大学 材料科学与工程学院, 吉林 长春 130022)

摘要: 采用顶部籽晶提拉法(TSSG)生长了钬铥双掺钨酸镱钾($KHo_{0.04}Tm_{0.06}Yb_{0.9}(WO_4)_2$)激光晶体。测试了该晶体的吸收及荧光光谱,计算了其光谱参数。实验结果表明:该晶体在890~1 000 nm范围吸收带较宽,半峰宽为90 nm,计算了主峰1 000 nm处吸收截面为16.92×10^{-20} cm^2;Tm^{3+}在1 690~1 812 nm范围存在较宽的吸收带,半峰宽为118 nm,易于实现Yb→Ho、Yb→Tm、Tm→Ho的能量传递。根据Judd-Ofelt理论,计算了该晶体的光谱强度参数。根据Tm^{3+}、Ho^{3+}、Yb^{3+}离子能级图,讨论了产生1 750~2 200 nm荧光发射的3种能量传递方式。最后计算了主峰2 030 nm处受激发射截面为3.47×10^{-20} cm^2,表明该晶体可作为2 μm波段优异的激光增益介质。

关 键 词: $KHo_{0.04}Tm_{0.06}Yb_{0.9}(WO_4)_2$激光晶体; 吸收光谱; 荧光光谱; 光谱参数计算

收稿日期: 2017-09-05; **修订日期**: 2017-10-24

基金项目: 吉林省科技发展计划(20160414043GH); 吉林省教育厅"十三五"科学技术研究项目(2016-379)资助
Supported by Jilin Provincial S&T Development Plan Project of China(20160414043GH); The 13th Five-year S&T Research Project of Jilin Provincial Education Department of China(2016-379)

1 Introduction

Ho^{3+}, Tm^{3+} ions can be commonly used as the activation ions at the range of 2 – 3 μm wavelength, which has the advantage of large stimulated-emission cross-section and long fluorescence lifetime. In the military, 2 μm laser has a strong ability to penetrate the smoke of the battlefield with good confidentiality. These two types of activation ions are suitable for military laser ranging, laser radar and electro-optical jamming, *etc*[1-4]. In the medical field, 2 μm laser can perform precise excision of biological tissues without damaging surrounding tissues, while reducing the anesthetic dosage[5]. In addition, it can be used to detect harmful gases such as formaldehyde with the magnitude of 10^{-9}, as well as carbon monoxide in the environment[6].

Tm^{3+} ions can be often used as the sensitizing agent of Ho^{3+} ions since Tm^{3+} ions have stronger absorption efficient than Ho^{3+} ions at the range of 785 – 810 nm. It can achieve the energy transfer of Tm→Ho and then improve the absorption efficiency to pumping light[7-11]. Yb^{3+} ions have been widely used as a sensitizing agent with the LD pumping popular. The absorption peak of Yb^{3+} ions located near 980 nm and can be effectively coupled with InGaAs LD. Because the energy level structure of Yb^{3+} ion is very simple without excitation state reabsorption process, Yb^{3+} can be served as the sensitizing agent of Ho^{3+}, Tm^{3+} ions.

$KYb(WO_4)_2$ is one of the self-activation laser crystals with a double tungstates structure. In the host of $KYb(WO_4)_2$, Yb^{3+} ions have been served as not only an integral part of the host, but also the active ions. The absorption wavelength of $KYb(WO_4)_2$ is 930 – 980 nm, which can be effectively coupled with the InGaAs LD pumping[12-14]. The laser output wavelength of $KYb(WO_4)_2$ is in the range of 980 – 1 080 nm. Laser emission with multi-wavelength and tenability in this crystal can be achieved by doping Er^{3+}, Tm^{3+}, Ho^{3+}, *etc*. *Re*:$KYb(WO_4)_2$ has several merits including high doping concentration, low fluorescence quenching, high conversion efficiency, low threshold value and well stability, *etc*. It can achieve all-solid-state, miniaturization and integration for lasers and widely used in the fields of human-eye safe, laser communication, medical treatment, remote sensing, *etc*[15-18]. In this paper, the growth, absorption and fluorescence spectra of $KHo_{0.04}Tm_{0.06}$-$Yb_{0.9}(WO_4)_2$ laser crystal were investigated, and the spectral parameters of this crystal were calculated as well.

2 Experiments

2.1 Crystal Growth

The chemicals included K_2CO_3(top-grade pure), Yb_2O_3(99.99%), Ho_2O_3(99.99%), Tm_2O_3(99.99%), and WO_3(99.999%). The $K_2W_2O_7$ was served as solvent. They were mixed and reacted based on the equations below:

$$0.04Ho_2O_3 + 0.06Tm_2O_3 + 0.9Yb_2O_3 + K_2CO_3 + 4WO_3 \rightarrow 2KHo_{0.04}Tm_{0.06}Yb_{0.9}(WO_4)_2 + CO_2, \quad (1)$$

$$K_2CO_3 + 2WO_3 \rightarrow K_2W_2O_7 + CO_2, \quad (2)$$

where the mole ratio of $KHo_{0.04}Tm_{0.06}Yb_{0.9}(WO_4)_2$ to $K_2W_2O_7$ was 1∶4. The crystal was grown by the Top Seeded Solution Growth (TSSG) method. The experimental equipment included a MCGE-furnace heated by resistance wire, a platinum crucible with a size of Φ60 mm × 50 mm, a Pt-Rh thermocouple, and an AI-808P thermal controller. The mixed materials was put in a platinum crucible and fully melted at a temperature of 80 ℃ above super-saturation for 24 h. The oriented crystallon was dipped at about 910 ℃, and grown gradually with a rotation rate of 15 r/min, a pulling rate of 2 mm/day and a cooling rate of 0.05/h. After 2 weeks, the crystal was removed from the crucible and cooled down to the room temperature at a rate of 20 ℃/h. Finally, the $KHo_{0.04}Tm_{0.06}Yb_{0.9}(WO_4)_2$ laser crystal with a dimension of 26 mm × 11 mm × 9 mm was obtained successfully. Then the crystal sample with a dimension of 3 mm × 3 mm × 1 mm was cut perpendicularly to *b* axis for spectral measurement.

2.2 Measurement of Sample

The absorption spectrum of the crystal sample was measured using an ultraviolet (UV) spectrophotometer(Model UV360, Shimadzu Company, Japan) at

room temperature. The fluorescence spectrum of the crystal sample was measured with an X-ray fluorescence spectrometer (FLUOROLOG-3, HORIBA Company, Japan) at room temperature.

3 Results and Discussion

3.1 Absorption Spectrum

The absorption spectrum of the crystal sample is shown in Fig. 1. There are several absorption peaks at 378, 421, 450, 475, 538, 625, 645, 691, 805, 890, 916, 980, 1 000, 1 190, 1 223, 1 690, 1 712, 1 749, 1 804, 1 812, 1 924 nm. It can be seen that the absorption peaks at 378, 475, 805 and 1 690 – 1 812 nm are accounting for $^3H_6 \rightarrow {}^1D_2(Tm^{3+})$, $^3H_6 \rightarrow {}^1G_4(Tm^{3+})$, $^3H_6 \rightarrow {}^3H_4(Tm^{3+})$ and $^3H_6 \rightarrow {}^3F_4(Tm^{3+})$ transitions, respectively. Meanwhile, the absorption peaks located at 421, 450, 538, 625 – 691, 890, 916, 1 190 (1 223), 1 924 nm are due to $^5I_8 \rightarrow {}^5G_5(Ho^{3+})$, $^5I_8 \rightarrow {}^5G_6(Ho^{3+})$, $^5I_8 \rightarrow {}^5F_4(Ho^{3+})$, $^5I_8 \rightarrow {}^5F_5(Ho^{3+})$, $^5I_8 \rightarrow {}^5I_4(Ho^{3+})$, $^5I_8 \rightarrow {}^5I_5(Ho^{3+})$, $^5I_8 \rightarrow {}^5I_6(Ho^{3+})$, $^5I_8 \rightarrow {}^5I_7(Ho^{3+})$ transitions, respectively. The absorption peaks at 981 and 1 000 nm are attributed to $^2F_{7/2} \rightarrow {}^2F_{5/2}(Yb^{3+})$ transition. The full width at half maximum (FWHM) at the range of 890 – 1 000 nm amounts to 90 nm, which is more propitious for InGaAs LD laser pumping. In this absorption spectrum, the most interesting is a broader absorption band (Tm^{3+}) at 1 690 – 1 812 nm with a FWHM of 118 nm. The effective energy transfer of Yb→Ho, Yb→Tm, Tm→Ho can be easily achieved to produce 2 μm around laser due to these two broader absorption bands at 890 – 1 000 nm (Yb^{3+}) and 1 690 – 1 812 nm (Tm^{3+}) in the crystal.

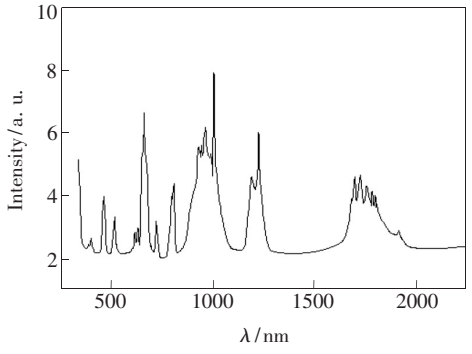

Fig. 1　Absorption spectrum of $KHo_{0.04}Tm_{0.06}Yb_{0.9}(WO_4)_2$ crystal

The absorption cross section σ_{abs} of the crystal can be defined as formula (3)[19]:

$$\sigma_{abs} = \frac{\int k(\lambda)\,d\lambda}{N} = \frac{D(\lambda)}{\lg e \cdot NL}, \qquad (3)$$

where D is the optical density, which can be calculated as $D = \lg(I_0/I)$, based on absorption spectrum measurements; I_0 and I represent the intensities of incident light and emergent light, respectively; N represents the concentration of Ho^{3+}, Tm^{3+} or Yb^{3+} ions, and L represents the thickness of the sample (L = 1 mm). The absorption cross section of the crystal at the strongest peak of 1 000 nm was calculated as 16.92×10^{-20} cm^2. Tab. 1 lists the main absorption peaks and absorption parameters of the crystal.

Meanwhile, the spectral intensity parameters in the crystal can be obtained based on the Judd-Ofelt theory[20-21] as follows: $\Omega_2 = 10.24 \times 10^{-20}$ cm^2, $\Omega_4 = 2.37 \times 10^{-20}$ cm^2, $\Omega_6 = 1.43 \times 10^{-20}$ cm^2.

Tab. 1　Main absorption peaks and absorption parameters of the $KHo_{0.04}Tm_{0.06}Yb_{0.9}(WO_4)_2$ crystal

Transition	λ/nm	N/cm^{-3}	σ_{abs}/cm^2
$^3H_6 \rightarrow {}^1D_2(Tm^{3+})$	378	2.94×10^{20}	1.17×10^{-20}
$^5I_8 \rightarrow {}^5G_5(Ho^{3+})$	421	1.96×10^{20}	0.92×10^{-20}
$^5I_8 \rightarrow {}^5G_6(Ho^{3+})$	450	1.96×10^{20}	3.38×10^{-20}
$^3H_6 \rightarrow {}^1G_4(Tm^{3+})$	475	2.94×10^{20}	2.12×10^{-20}
$^5I_8 \rightarrow {}^5F_4(Ho^{3+})$	538	1.96×10^{20}	3.89×10^{-20}
$^5I_8 \rightarrow {}^5F_5(Ho^{3+})$	625	1.96×10^{20}	1.93×10^{-20}
	645	1.96×10^{20}	1.95×10^{-20}
	691	1.96×10^{20}	4.47×10^{-20}
$^3H_6 \rightarrow {}^3H_4(Tm^{3+})$	805	2.94×10^{20}	3.28×10^{-20}
$^5I_8 \rightarrow {}^5I_4(Ho^{3+})$	890	1.96×10^{20}	5.32×10^{-20}
$^5I_8 \rightarrow {}^5I_5(Ho^{3+})$	916	1.96×10^{20}	7.89×10^{-20}
$^2F_{5/2} \rightarrow {}^2F_{5/2}(Yb^{3+})$	980	4.4×10^{21}	15.27×10^{-20}
	1 000	4.4×10^{21}	16.92×10^{-20}
$^5I_8 \rightarrow {}^5I_6(Ho^{3+})$	1 190	1.96×10^{20}	5.31×10^{-20}
	1 223	1.96×10^{20}	5.46×10^{-20}
$^3H_6 \rightarrow {}^3F_4(Tm^{3+})$	1 690 – 1 812	2.94×10^{20}	10.35×10^{-20}
$^5I_8 \rightarrow {}^5I_7(Ho^{3+})$	1 924	1.96×10^{20}	3.02×10^{-20}

3.2 Fluorescence Spectrum

The fluorescence spectrum of the crystal sample

under 980 nm pumping is shown in Fig. 2. There are four obvious emission peaks at 950 – 1 050 nm, 1 100 – 1 250 nm, 1 400 – 1 470 nm, 1 750 – 2 200 nm, which are attributed to $^2F_{5/2} \rightarrow {}^2F_{7/2}$ (Yb^{3+}), $^3H_5 \rightarrow {}^3H_6$ (Tm^{3+}) & $^5I_6 \rightarrow {}^5I_8$ (Ho^{3+}), $^3H_4 \rightarrow {}^3F_4$ (Tm^{3+}), $^3F_4 \rightarrow {}^3H_6$ (Tm^{3+}) & $^5I_7 \rightarrow {}^5I_8$ (Ho^{3+}) transitions, respectively. The emission line width at 1 750 – 2 200 nm amounts to 250 nm, which is due to the overlap between $^3F_4 \rightarrow {}^3H_6$ (Tm^{3+}) and $^5I_7 \rightarrow {}^5I_8$ (Ho^{3+}). It is indicated that the crystal can be used as a high quality tunable laser medium at 2 μm.

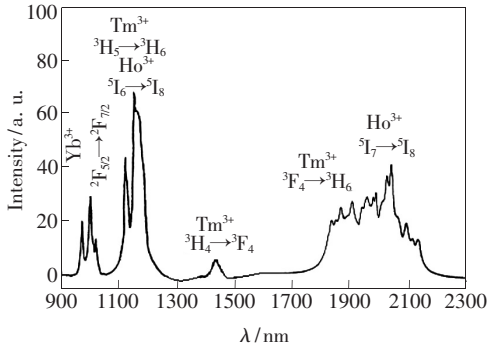

Fig. 2 Fluorescent spectrum at 900 – 2 300 nm of the $KHo_{0.04}Tm_{0.06}Yb_{0.9}(WO_4)_2$ crystal

The energy level diagram sketched in Fig. 3 can describe the energy transfer among Tm^{3+}, Yb^{3+}, Ho^{3+} ions in the crystal. The fluorescence emission at 1 750 – 2 200 nm is due to the following three energy transmission interaction.

(1) Energy transfer of $Yb^{3+} \rightarrow Tm^{3+}$

Yb^{3+} ions can uptake quantities of pumping light to generate $^2F_{7/2} \rightarrow {}^2F_{5/2}$ absorption transition under 980 nm excitation. Then the energy was transferred from $^2F_{5/2}$ (Yb^{3+}) to $^3H_6$ (Tm^{3+}) and $^3H_6 \rightarrow {}^3H_5$ transition of Tm^{3+} ions can be achieved. From $^3H_5$ energy state (Tm^{3+}), the emission at 1 700 – 1 900 nm ($^3F_4 \rightarrow {}^3H_6$) can be obtained by the non-radiative transition process from $^3H_5$ to $^3F_4$ energy state.

(2) Energy transfer of $Yb^{3+} \rightarrow Ho^{3+}$

Yb^{3+} ions generate a $^2F_{7/2} \rightarrow {}^2F_{5/2}$ absorption transition due to the 980 nm excitation. Then the energy is transferred from $^2F_{5/2}$(Yb^{3+}) to $^5I_8$(Ho^{3+}) and $^5I_8 \rightarrow {}^5I_6$ transition of Ho^{3+} ions can be achieved. From $^5I_6$ energy state (Ho^{3+}), the emission at 1 900 – 2 200 nm($^5I_7 \rightarrow {}^5I_8$) can be obtained by the non-radiative transition process from $^5I_6$ to $^5I_7$ energy state.

(3) Energy transfer of $Tm^{3+} \rightarrow Ho^{3+}$

This efficient resonant energy transfer happens due to the energy approximate overlap between the $^3F_4$(Tm^{3+}) and $^5I_7$(Ho^{3+}) energy levels. Therefore, the emission at 1 900 – 2 200 nm ($^5I_7 \rightarrow {}^5I_8$) can be achieved based on the energy transfer from $^3F_4$(Tm^{3+}) to $^5I_7$(Ho^{3+}).

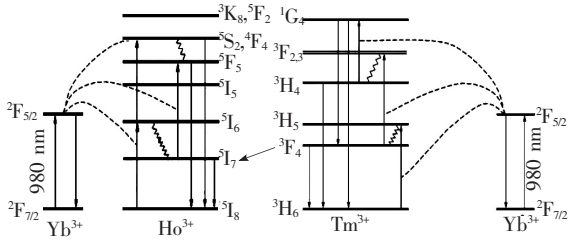

Fig. 3 Energy level diagram of Tm^{3+}, Yb^{3+}, Ho^{3+} ions and emission channels.

According to the formula (4)[15], the stimulated emission cross section of main emission peak at 2 030 nm can be calculated as 3.47×10^{-20} cm^2.

$$\sigma_{em}(\lambda) = \frac{\lambda^4 I(\lambda)}{8\pi n^2 c \tau_f \int I(\lambda)\,d\lambda}, \qquad (4)$$

where λ represents the fluorescent wavelength (λ = 2 030 nm), n refers to the refractive index (n = 2.17), c represents the light speed in the vacuum ($c = 3 \times 10^8$ m/s), τ_f is the spontaneous fluorescence time ($\tau_f = 1.8$ ms). $I(\lambda)/\int I(\lambda)\,d\lambda$ can be defined as the normalized line shape function, corresponding to $^5I_7 \rightarrow {}^5I_8$ transition of Ho^{3+} ions.

4 Conclusion

$KHo_{0.04}Tm_{0.06}Yb_{0.9}(WO_4)_2$ laser crystal with a dimension of 26 mm × 11 mm × 9 mm was grown by the TSSG method. The testing result of absorption spectrum shows that Yb^{3+} ions have a wider absorption band at the range of 890 – 1 000 nm with a FWHM of 90 nm, and Tm^{3+} ions have a broader absorption band at 1 690 – 1 812 nm with a FWHM of 118 nm. The effective energy transfer of Yb→Ho, Yb→Tm, Tm→Ho can be easily achieved to produce 2 μm around laser due to these two broader

absorption bands at 890 – 1 000 nm (Yb^{3+}) and 1 690 – 1 812 nm (Tm^{3+}) in the crystal. The fluorescent spectrum measurement result indicates that the emission line width at 1 750 – 2 200 nm amounts to 250 nm, which is due to the overlap between $^3F_4 \rightarrow {}^3H_6$ (Tm^{3+}) and $^5I_7 \rightarrow {}^5I_8$ (Ho^{3+}). The spectral strength parameters of the crystal were calculated based on the Judd-Ofelt theory as follows: $\Omega_2 = 10.24 \times 10^{-20}\,cm^2$, $\Omega_4 = 2.37 \times 10^{-20}\,cm^2$, $\Omega_6 = 1.43 \times 10^{-20}\,cm^2$. According to the energy level diagram of Tm^{3+}, Ho^{3+} and Yb^{3+} ions, three kinds of energy transfer modes at 1 750 – 2 200 nm emission were discussed in the crystal. The stimulated emission cross section of main emission peak at 2 030 nm is $3.47 \times 10^{-20}\,cm^2$. It is indicated that $KHo_{0.04}Tm_{0.06}Yb_{0.9}(WO_4)_2$ laser crystal can be widely used as an excellent laser gain medium at 2 μm around wavelength.

References:

[1] 袁云松, 吴从越, 李雨芬, 等. 铥、镱共掺可见光响应型纳米 TiO_2 光催化剂的制备及性能表征 [J]. 发光学报, 2016, 37(11):1310-1315.
YUAN Y S, WU C Y, LI Y F, *et al.*. Preparation and characterization of TiO_2: Tm, Yb visible light responsive nano-photocatalyst [J]. *Chin. J. Lumin.*, 2016, 37(11):1310-1315. (in Chinese)

[2] 孙超, 朱忠丽, 张莹. 低温燃烧法制备的 Ho: YbGG 多晶粉体及其发光性能 [J]. 发光学报, 2014, 35(9): 1065-1070.
SUN C, ZHU Z L, ZHANG Y. Ho: YbGG polycrystal powder synthesized by low temperature combustion method and its luminescent characteristics [J]. *Chin. J. Lumin.*, 2014, 35(9):1065-1070. (in Chinese)

[3] 付作岭, 董晓睿, 盛天琦, 等. 纳米晶体中稀土离子的发光性质及其变化机理研究 [J]. 中国光学, 2015, 8(1): 139-144.
FU Z L, DONG X R, SHENG T Q, *et al.*. Luminescene properties and various mechanisms of rare earth ions in the nanocrystals [J]. *Chin. Opt.*, 2015, 8(1):139-144. (in Chinese)

[4] 任国光, 黄裕年. 用激光红外干扰系统保护军用和民航机 [J]. 激光与红外, 2006, 36(1):1-6.
REN G G, HUANG Y N. Laser-based IRCM system defenses for military and commercial aircraft [J]. *Laser & Infrared*, 2006, 36(1):1-6. (in Chinese)

[5] VODOPYANOV K L, STAFSUDD R. Generation of *Q*-switched Er: YAG laser pulse evanescent wave absorption in ethanol [J]. *Appl. Phys. Lett.*, 1998, 72:2211.

[6] SRINIVASAN B, TAFOYA J, JAIN R K. High-power "watt-level" CW operation of diode-pumped 2.7 μm fiber laser using efficient cross-relaxation and energy transfer mechanisms [J]. *Opt. Experess*, 1999, 4:495.

[7] REMSKI R, JAMES L T, GOOEN K H. Pulsed laser action in $LiYF_4$: Er^{3+}, Ho^{3+} at 77 K [J]. *IEEE Quant. Electron.*, 1969, 5(4):214.

[8] IMAI S, YAMADA T, FUJIMORI Y, *et al.*. A 20 W Cr^{3+}, Tm^{3+}, Ho^{3+}: YAG laser [J]. *Opt. Laser Technol.*, 1990, 22(5):351-353.

[9] 姚宝权, 董力强, 王月珠, 等. 激光二极管抽运 Tm, Ho: YLF 微片激光器的实验研究 [J]. 光学学报, 2004, 24(1):79-83.
YAO B Q, DONG L Q, WANG Y Z, *et al.*. Experimental study of microchip (Tm, Ho): YLF laser pumped by laser diode [J]. *Acta Opt. Sinica*, 2004, 24(1):79-83. (in Chinese)

[10] 何晓敏, 张新陆, 王月珠, 等. 激光二极管泵浦室温 Tm, Ho: YLF 微片激光器的实验研究 [J]. 激光与红外, 2005, 35(9):367-340.
HE X M, ZHANG X L, WANG Y Z, *et al.*. Experimental study of laser-diode pumped room temperature Tm, Ho: YLF microchip laser [J]. *Laser & Infrared*, 2005, 35(9):367-340. (in Chinese)

[11] 张兴宝, 姚宝权, 王月珠, 等. 准四能级双掺 Tm/Ho 钒酸钆激光器 [J]. 激光技术, 2006, 30(2):119-122.
ZHANG X B, YAO B Q, WANG Y Z, *et al.*. Quasi-four-level co-doped Tm/Ho gadolinium vanadate laser [J]. *Laser Technol.*, 2006, 30(2):119-122. (in Chinese)

[12] BRENIER A. A new evaluation of Yb^{3+}-doped crystals for laser applications [J]. *J. Lumin.*, 2001, 92:199-201.

[13] 张莹, 刘景和, 李春, 等. 高浓度铒离子掺杂钨酸镱钾激光晶体上转换发光研究 [J]. 激光与红外工程, 2012, 41(9):2322-2327.
ZHANG Y, LIU J H, LI C, *et al.*. Up-conversion luminescence of highly Er^{3+}-doped potassium ytterbium tungstate laser crystal [J]. *Infrared Laser Eng.*, 2012, 41(9):2322-2327. (in Chinese)

[14] KLOPP P, GRIEBNER U, PETROV V, *et al.*. Laser operation of the new stoichiometric crystal $KYb(WO_4)_2$ [J]. *Appl. Phys.* B, 2002, 74:185-189.

[15] MATEOS X, PUJOL M C, GÜELL F, *et al.*. Sensitization of Er^{3+} emission at 1.5 μm by Yb^{3+} in $KYb(WO_4)_2$ single crystals [J]. *Phys. Rev.* B, 2002, 66:214104.

[16] LOIKO P A, VILEJSHIKOVA E V, MATEOS X, *et al.*. Europium doping in monoclinic $KYb(WO_4)_2$ crystal [J]. *J. Lumin.*, 2017, 183:217-225.

[17] LOIKO P, MATEOS X, DUNINA E, *et al.*. Judd-Ofelt modelling and stimulated-emission cross-sections for Tb^{3+} ions in monoclinic $KYb(WO_4)_2$ crystal [J]. *J. Lumin.*, 2017, 190:37-44.

[18] 王宇明, 张礼杰, 雷鸣, 等. 泡生法生长 $KYb(WO_4)_2$ 晶体及其结构与光谱性能 [J]. 中国激光, 2006, 33(5):697-700.
WANG Y M, ZHANG L J, LEI M, *et al.*. Structure and spectra characteristics of $KYb(WO_4)_2$ crystal grown by Kyropoulos method [J]. *Chin. J. Lasers*, 2006, 33(5):697-700. (in Chinese)

[19] SARDAR D K, RUSSELL CC, YOW R M, *et al.*. Spectroscopic analysis of the Er^{3+} ($^4f_{11}$) absorption intensities in $NaBi(WO_4)_2$ [J]. *Appl. Phys.*, 2004, 95(31):1180-1184.

[20] JUDD B R. Optical absorption intensities of rare-earth ions [J]. *Phys. Rev.*, 1962, 127:750.

[21] OFELT G S. Intensities of crystal spectra of rare earth ions [J]. *J. Chem. Phys.*, 1962, 37:511.

毕琳(1984 -),女,吉林松原人,博士,讲师,2016 年于中国科学院大学获得博士学位,主要从事计算机应用、计算机模拟仿真等方面的研究。
E-mail: bilin7080@163.com